



Supplement of

Observed water and light limitation across global ecosystems

François Jonard et al.

Correspondence to: François Jonard (francois.jonard@uliege.be)

The copyright of individual parts of the supplement might differ from the article licence.

S1. MODIS NDVI time series and mean climatology for two example pixels

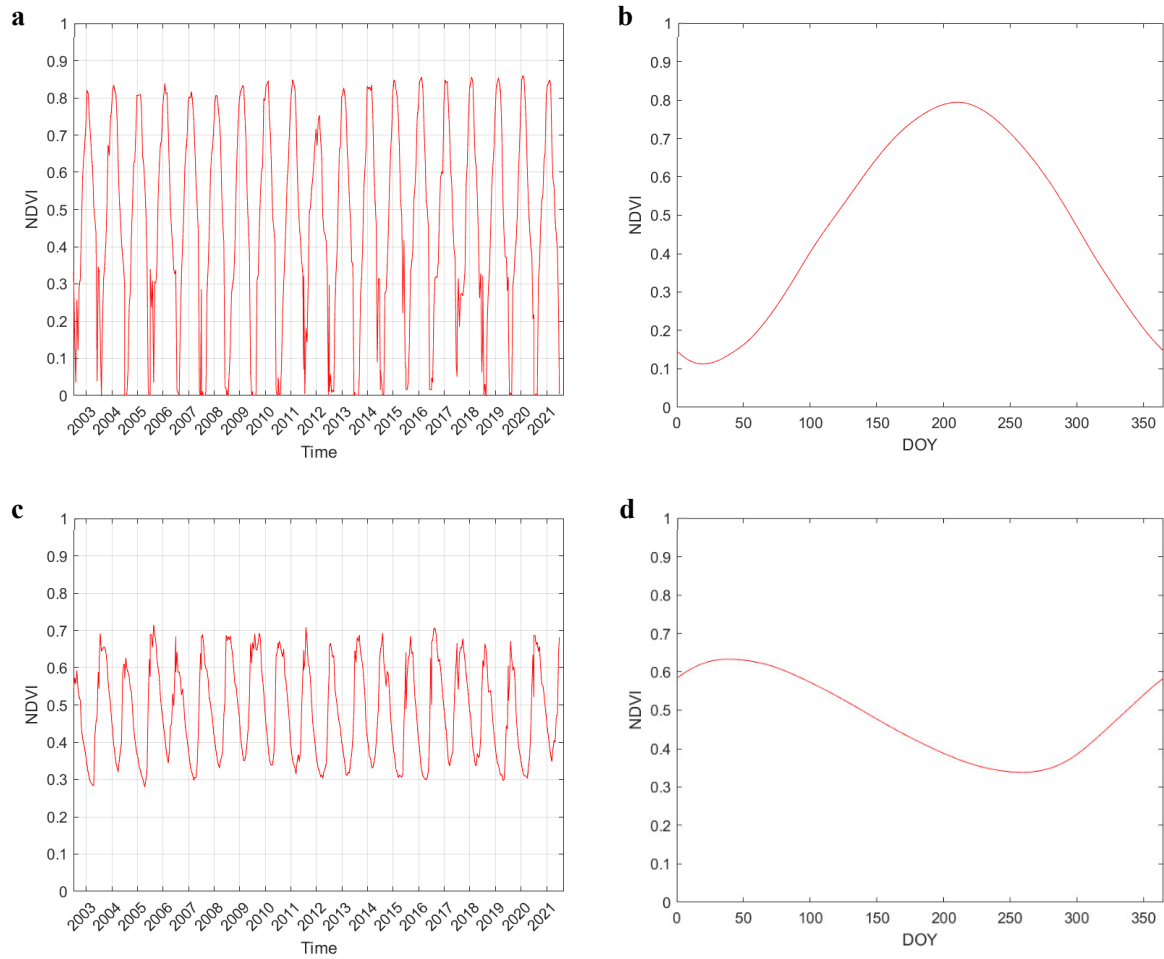


Figure S1. MODIS NDVI time series (a,c) and mean climatology (b,d) for two representative locations. (a,b) Pixel in the US Corn Belt region showing a phenological peak on DOY 211. (c,d) Pixel in southern Africa (Zimbabwe) showing a phenological peak on DOY 39.

S2. SM-PAR growing-season correlation

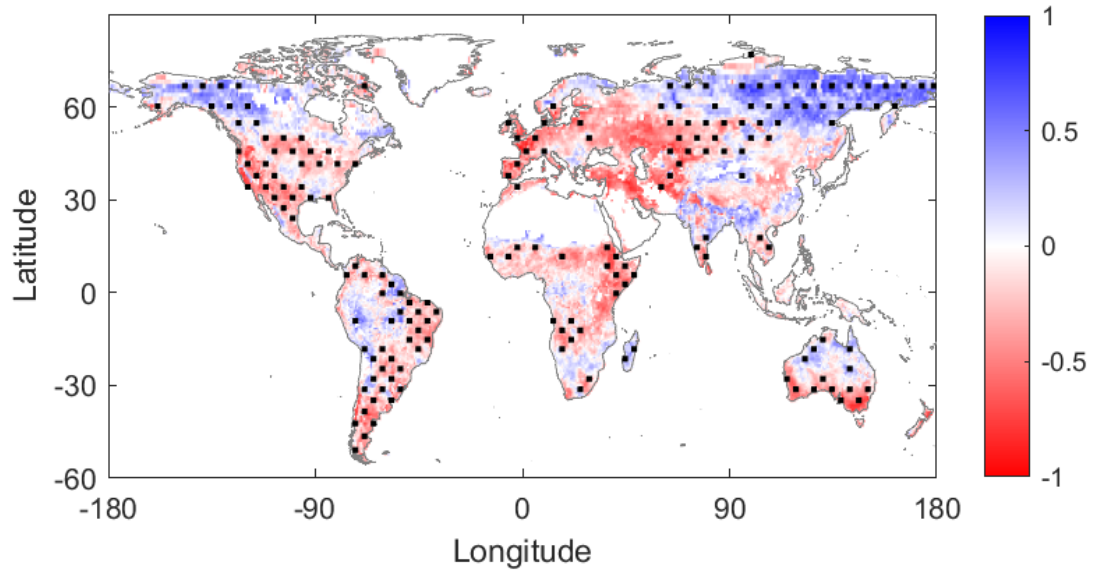


Figure S2. Growing-season Pearson correlation coefficient between SMAP soil moisture (SM) and MERRA-2 photosynthetically active radiation (PAR). Regions of statistical significance ($P < 0.05$) are indicated with stippling.

S3. Spatial distribution of the model threshold

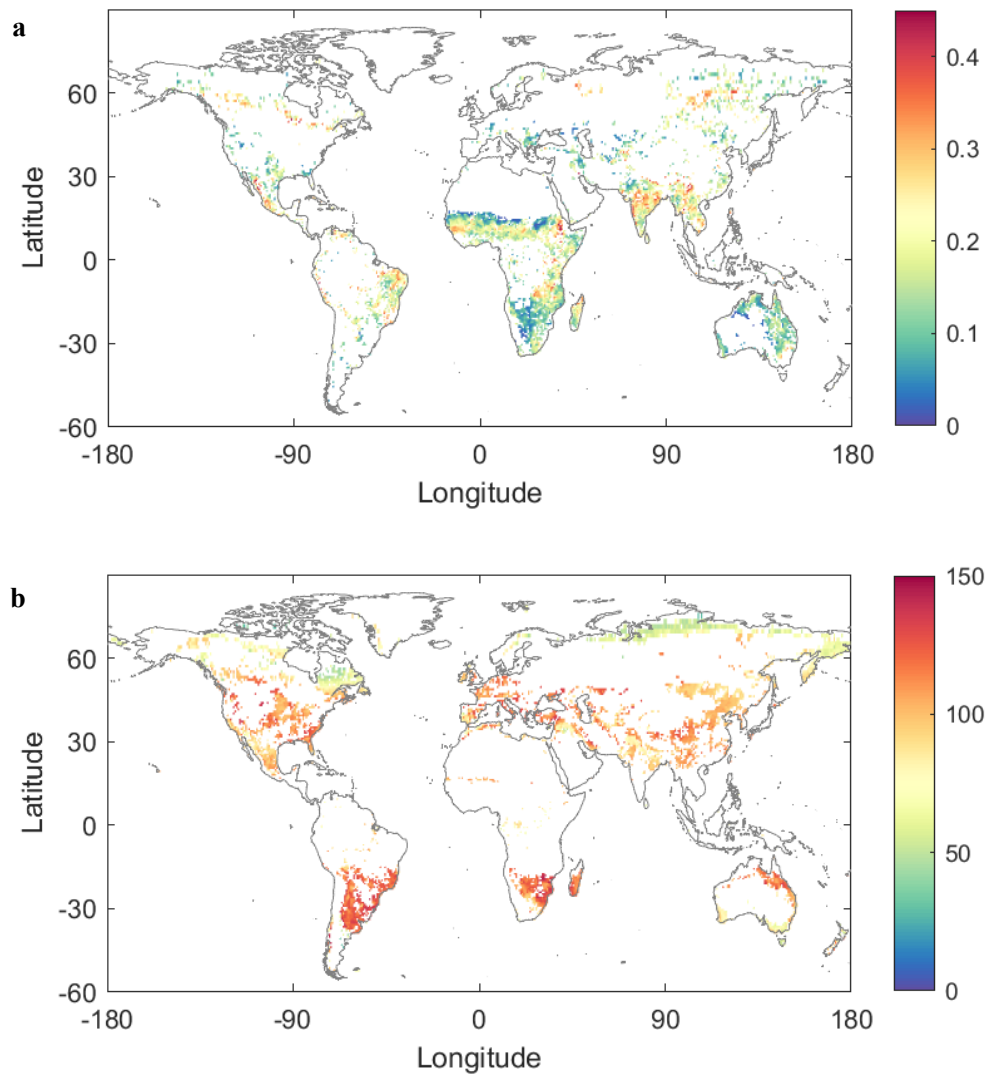


Figure S3. Spatial distribution of the model threshold for the (a) SIF-SM ($\text{m}^3 \text{m}^{-3}$) and (b) SIF-PAR (W m^{-2}) relationships. White shading denotes areas where the SIF-SM or SIF-PAR correlation is not positive—i.e., where SIF is not increasing with SM/PAR—or areas where no collocated SIF and SM/PAR records are available.

S4. Model threshold as a function of vegetation type

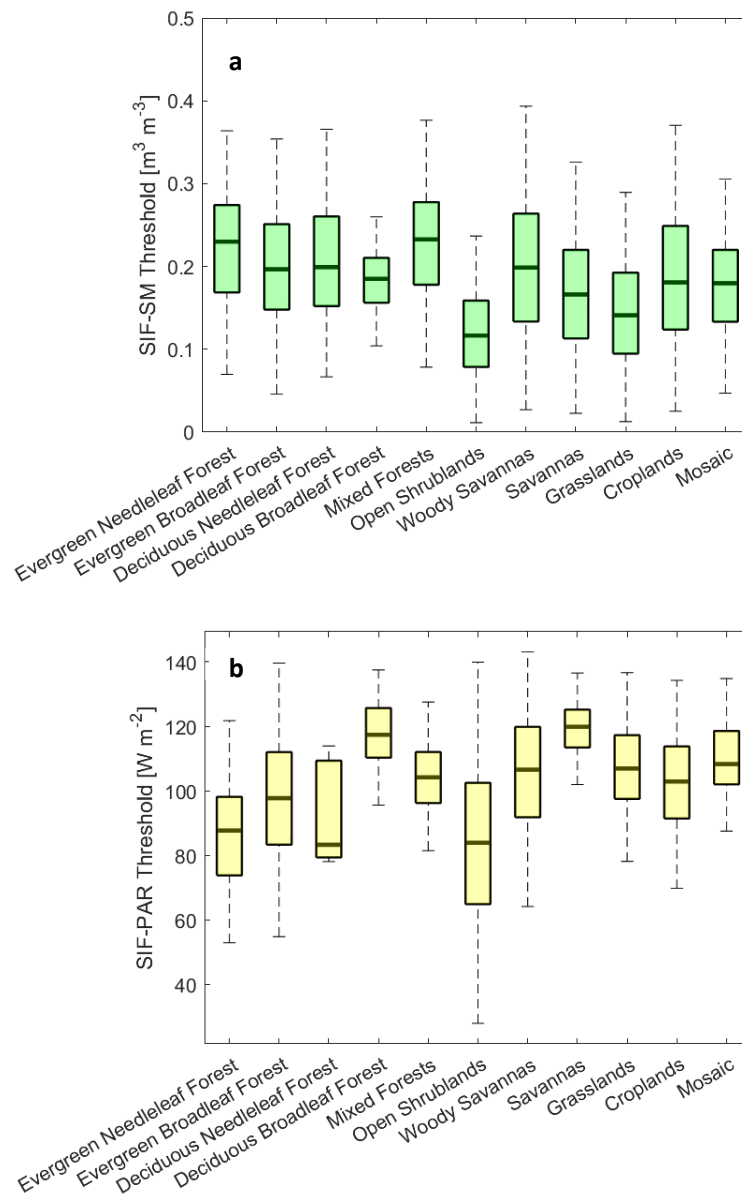


Figure S4. (a) SIF-SM model threshold ($\text{m}^3 \text{m}^{-3}$) and (b) SIF-PAR model threshold (W m^{-2}) binned as a function of vegetation type based on International Geosphere-Biosphere Program (IGBP) land cover classification. Box edges are the 25th and 75th percentiles of the distribution bounding the median (bold line), and whiskers extend to extrema (maximum and minimum). Only IGBP classes with more than 200 data points are shown.

S5. Spatial distribution of model type, slope, and threshold based on GOME2 SIF data

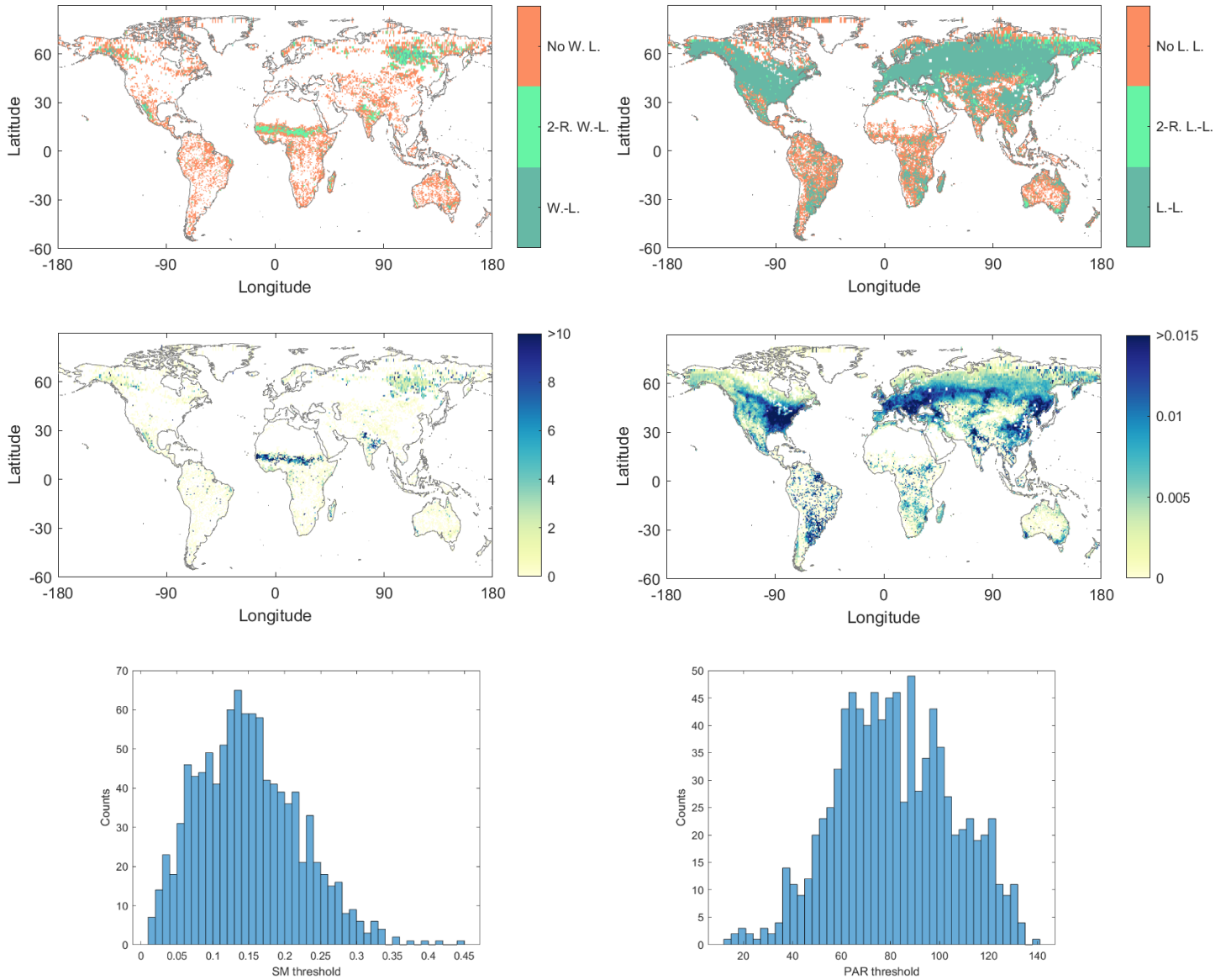


Figure S5. Estimated SIF-soil moisture (left column) and SIF-photosynthetically active radiation (right column) relationship features based on SIF data ($\text{mW m}^{-2} \text{nm}^{-1} \text{sr}^{-1}$) obtained from the Global Ozone Monitoring Experiment-2 (GOME-2) instrument aboard the MetOp-A satellite. Retrievals of SIF were obtained at 740 nm using the method proposed by Joiner et al. (2013) for a 4-year period from April 2015 to March 2019. Same format as Figs. 6 and 7.

S6. Coefficient of determination and coefficient of variation of the model fit

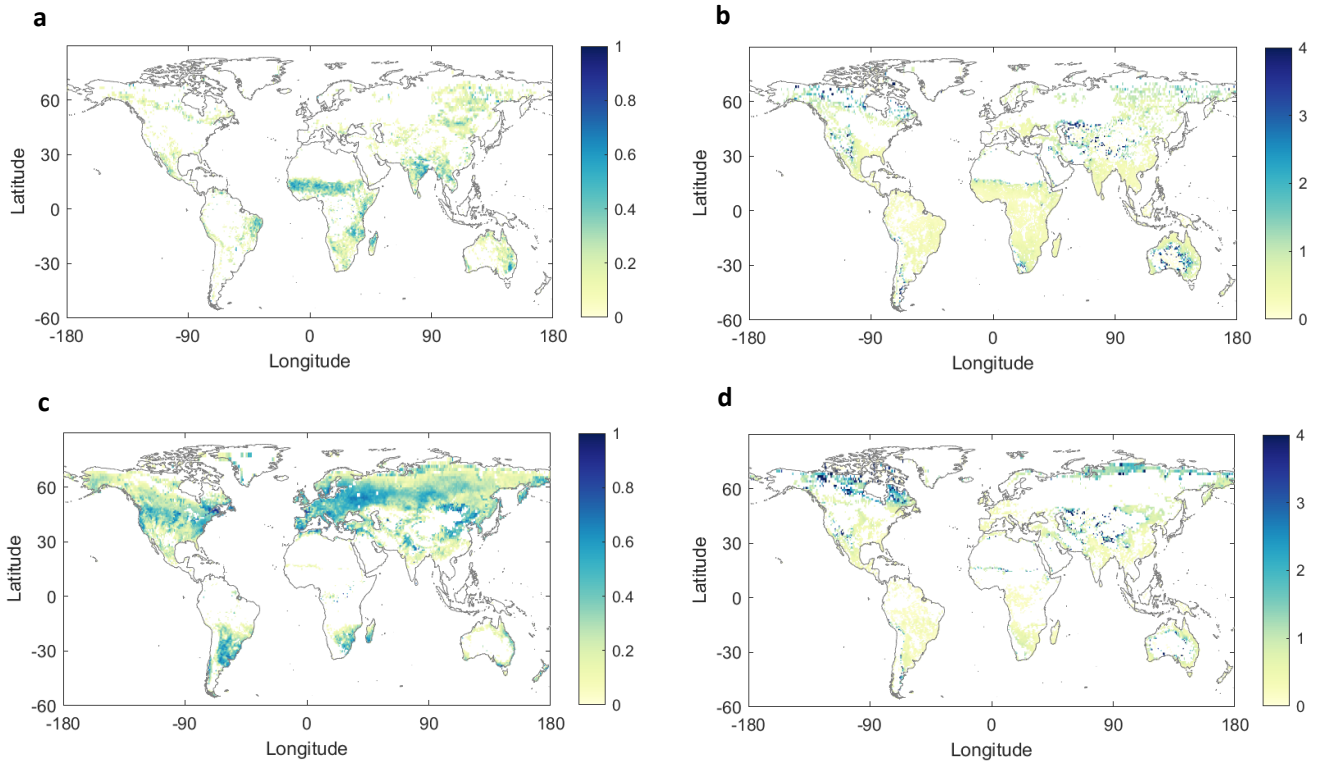


Figure S6. Coefficient of determination (R^2) and coefficient of variation (CV) of the model fit. The coefficient of determination is calculated for pixels in water- (a) or light- (c) limited conditions (i.e., linear model and sloped part of the two-regime model), while the coefficient of variation is calculated for pixels in non-limited water (b) or light (d) conditions (constant part of the two-regime model and zero-slope model) where R^2 has no meaningful definition.

S7. SIF-SM maps considering a shorter growing season defined using an NDVI threshold of 75%

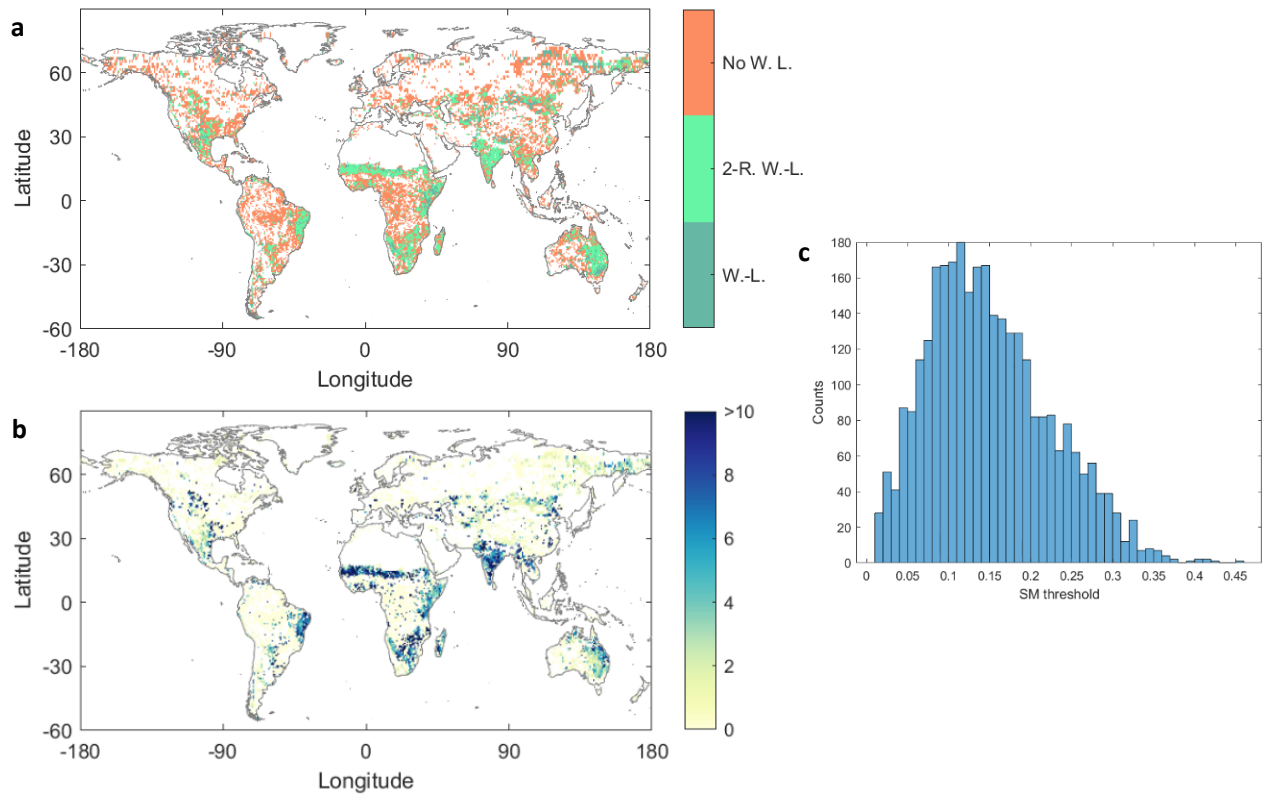


Figure S7. Estimated SIF-soil moisture relationship features based on a shorter growing season defined using an NDVI threshold of 75%. (a) Model type (W.-L.: water-limited; 2-R. W.-L.: two-regime water-limited; No W. L.: no water limitation), (b) model slope ($\text{mW m}^{-2} \text{nm}^{-1} \text{sr}^{-1}$) in the water-limited regime, and (c) model threshold ($\text{m}^3 \text{m}^{-3}$) for the SIF-SM relationship. Same format as Figs. 6 and 7.

S8. SIF-PAR maps considering a shorter growing season defined using an NDVI threshold of 75%

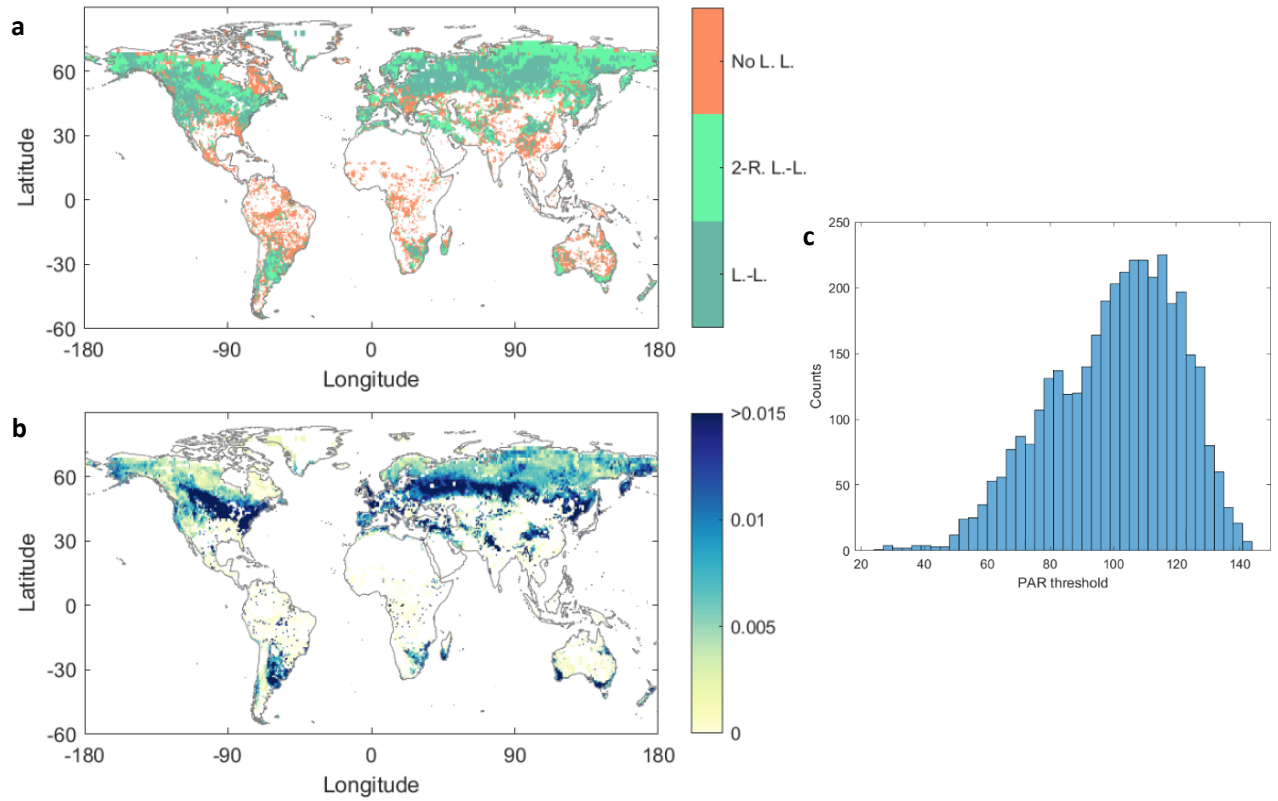


Figure S8. Estimated SIF-photosynthetically active radiation relationship features based on a shorter growing season defined using an NDVI threshold of 75%. (a) Model type (L.-L.: light-limited; 2-R. L.-L.: two-regime light-limited; No L. L.: no light limitation), (b) model slope ($10^{-3} \text{ nm}^{-1} \text{ sr}^{-1}$) in the light-limited regime, and (c) model threshold (W m^{-2}) for the SIF-PAR relationship.

S9. Bootstrapping analysis for two example pixels

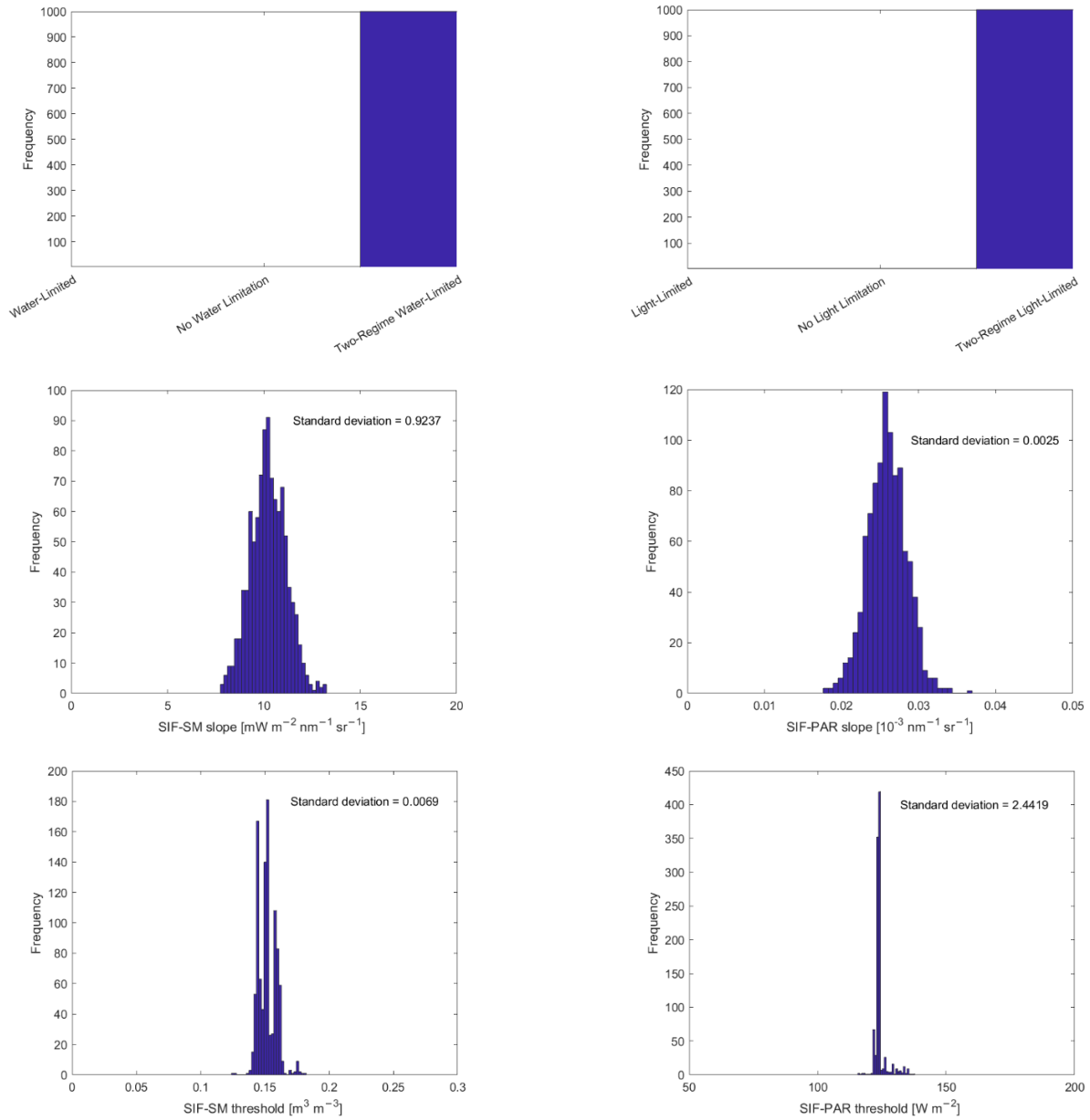


Figure S9. Uncertainty analysis of the model selection, model slope, and model threshold using bootstrapping (1000 iterations) for two representative locations. Left column: pixel in the Central African Republic (latitude/longitude: 9.65°N/22.78°E) showing a two-regime water limitation. Right column: pixel in Argentina (latitude/longitude: 32.79°S/63.11°W) showing a two-regime light limitation.